Available online at www.sciencedirect.com
SCIENCE DIRECT®
Thermochimica Acta 419 (2004) 195–204
thermochimica acta
www.elsevier.com/locate/tca

Advances in jewellery microcasting

Patrizio Sbornicchia [a,*], Giampiero Montesperelli [b], Gabriel M. Ingo [c], Gualtiero Gusmano [a]

[a] *University of Rome Tor Vergata, Via della Ricerca Scientifica, Rome 00133, Italy*
[b] *Polytechnic University of Marche, Via Brecce Bianche, Ancona 60131, Italy*
[c] *C.N.R., I.S.M.N., Monterotondo Station, 00016 CP 10 Rome, Italy*

Received 10 June 2003; received in revised form 4 December 2003; accepted 7 December 2003

Available online 13 February 2004

Abstract

Traditional moulds for jewellery casting are made of SiO_2 refractory particles agglomerated by a bonding phase. Typical precious alloys are moulded around 1100 °C, a temperature that might lead to partial thermal decomposition of the bonding phase, typically $CaSO_4$. The degradation process usually causes release of gas, e.g. SO_x, which is responsible for high porosity and roughness in the casting. These gas imperfections are responsible for about 10% of the overall casting failures.

The study of novel bonding phases, developed to eliminate gas defects and improve mechanical strength, is reported in this paper. In traditional moulds, bonding is generated during the investment stage, the new phases are obtained during ceramic burnout. New moulds are made from a mixture of quartz and CaO powders, and in the investment stage, quartz particles are embedded in a network of $Ca(OH)_2$. In the next firing, $Ca(OH)_2$ first dehydrates and then reacts with the surface of SiO_2 particles to form Ca_xSiO_{x+2} phases. These interfacial compounds provide a refractory scaffold for SiO_2.

The process has been studied by TG–DTA. Different firing temperatures have been tested and the silicate moulds have been studied by XRD. Mechanical and casting performances have been evaluated by compression tests and microstructural analysis. Cast comparison with respect to the traditional refractory is also illustrated.

Keywords: Jewellery casting; Lost wax casting; Refractory shells; Precious alloys; Metal gas porosity; Ceramic investment

1. Introduction

The moulding of metals stretches back to the Bronze age. Gold castings appeared during the Babylonian period (2600 B.C.) together with the lost wax method [1]. This technique reached a high degree of excellence, as attested by many beautiful and finely detailed statues, jewellery and artefacts from antiquity.

Nevertheless, modern industry ignored lost wax casting until the work of D. Philbrook in Iowa (1897) and William H. Taggart in Chicago (1907), when it was adopted by dentistry for producing crowns and inlays [2]. Further, improvements were achieved after the Second World War, by introduction of rubber moulds for serial production of wax models and cristobalite as a refractory that offsets the shrinkage of gold alloys [2].

The current technique requires a wax model and its investment through hardening of a refractory slurry. The raw material for jewellery casts traditionally consists of a mixture of silica (SiO_2) and hemihydrated calcium sulphate ($CaSO_4{\cdot}(1/2)H_2O$) powders. This undergoes an investment stage as follows. The addition of water causes precipitation of gypsum $CaSO_4{\cdot}2H_2O$ crystals, which acts as a scaffold for the refractory SiO_2 particles after slurry setting. A dewaxing and burnout cycle in an oven follows the investment stage. Burnout removes water of crystallization from the mould, thus avoiding alloy ejection during casting [3,4]. Finally, molten alloys are poured into the previously fired moulds.

Most jewellery manufacturing requires lost wax casting, which reliably provides high resolution of details and reproducibility of complex shapes. The use of the traditional refractory is cheap and good quality artefacts may be obtained, but many castings must be scraped. Defects can be caused by the gas, principally SO_3, produced by thermal decomposition of $CaSO_4$ or by the low mechanical strength of

* Corresponding author. Tel.:+39-06-72594273; fax: +39-06-72594328.
E-mail address: sbornicchia@scienze.uniroma2.it (P. Sbornicchia).

0040-6031/$ – see front matter © 2004 Elsevier B.V. All rights reserved.
doi:10.1016/j.tca.2003.12.017

the bonding phase [5]. About 10% of the rejects come from porosity flaws [6]. Elimination of casting defects typically requires expensive finishing treatments.

To improve thermal stability and mechanical strength of moulds, a new formulation with a quartz refractory phase and Ca_xSiO_{x+2} as bonding has been developed. Silicate moulds show much greater thermal stability and adhesion than traditional moulds and can reach temperatures as high as 1400 °C without chemical transformation. In traditional moulds, $CaSO_4$ anhydrite decomposition occurs at 1026 °C, i.e. just within the range of jewellery casting (T = 900–1200 °C) for gold and silver alloys. Thermochemical and mechanical properties of silicate moulds are compared with traditional moulds in this study. The effect of SiO_2/CaO ratio and of different firing temperatures on thermal and mechanical features of silicate moulds are evaluated. Finally, casting tests were carried out with Ag alloy, to evaluate the quality of final products.

2. Experimental

Traditional moulds were prepared from a commercial mixture (Randolf, Ultravest®), 75 wt.% SiO_2 (α-quartz and α-cristobalite) and 25 wt.% $CaSO_4{\cdot}(1/2)H_2O$. The slurry was set by addition of 40 ml of distilled water per 100 g of mixture. Burnout was done following the manufacturer's directions, firing at 730 °C for 5 h after heating at a rate of 2 °C min^{-1}.

New moulds were prepared with two different SiO_2/CaO ratios, 75 wt.% SiO_2 α-quartz (99.7 wt.%, Fluka) and 25 wt.% CaO (98 wt.%, Aldrich), and 80 wt.% α-quartz and 20 wt.% CaO. Both compositions were mixed in a rotary mixer. Slurries were achieved by adding, respectively, 48.0 and 43.0 ml of distilled water per 100 g of powder.

To evaluate the effect of the firing temperature on phases, microstructural modifications and the related mechanical and casting performances, samples were heated at 1000 or 1200 °C for 1 h, at a heating raxte of 2 °C min^{-1}. Thermal stability was studied by TG–DTA analysis (Netsch STA 409) in the temperature range between 25 and 1400 °C in air flow (80 sccm). Microstructural characterisation was been evaluated by SEM–EDS (Cambridge Stereoscan 360-Oxford EXL II) and X-ray diffraction (X-Pert Pro Philips with copper anode).

Mechanical tests were performed with an MTS 858 Minibionix (Instron) press under strain control (0.5 mm min^{-1}) according to ASTM (C133) standards. Porosity measurements were carried out by mercury intrusion on Porosimeter 2000 (Carlo Erba Instruments) equipped with a macropores unit. Five samples from each experimental condition were tested.

Wax models were made of Ruby Red wax (Kerr) typically used for jewellery investments. The models were a disk 15 mm in diameter and 2 mm thick. The models were invested by slurries in a cylindrical container, to produce moulds 30 mm in diameter and 35 mm tall.

Molten Ag 800 (80 wt.% Ag, 20 wt.% Cu) alloy was used to test the casting performance of the silicate moulds. The silver alloy was prepared by dissolving 20 g of electrolytic copper into 80 g of molten Ag (99.99%) at 1100 °C. The liquid alloy was cast into both traditional and silicate dewaxed moulds held at 400 °C. Optical and SEM microscopy were used to investigate the surface microstructure of the cast alloys.

3. Results and discussion

An SEM micrograph of a green traditional mould is shown in Fig. 1. The microstructure is a mixture of SiO_2 particles of

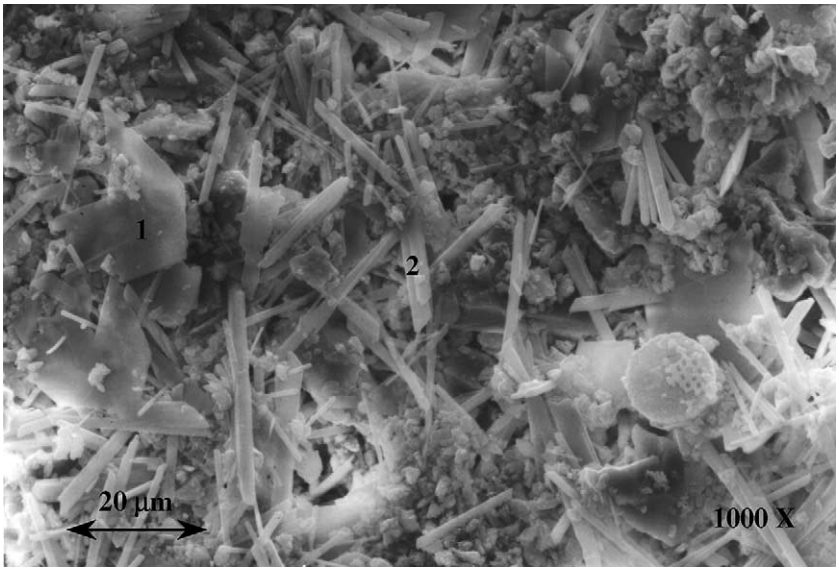

Fig. 1. SEM micrograph of traditional green mould: (1) SiO_2; (2) $CaSO_4{\cdot}2H_2O$.

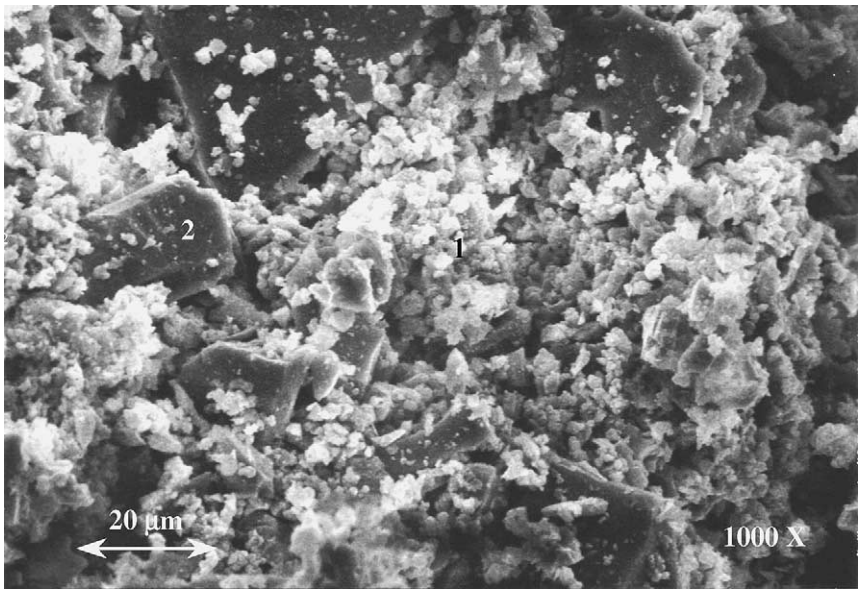

Fig. 2. SEM micrograph of green mould containing 25 wt.% CaO: (1) $Ca(OH)_2$; (2) α-quartz SiO_2.

15–20 μm, linked by $CaSO_4{\cdot}2H_2O$ needles, 10–25 μm long. An SEM micrograph of green mould, containing 25 wt.% CaO, after addition of water and setting, is shown in Fig. 2. Water addition to the SiO_2–CaO mixture leads to precipitation of $Ca(OH)_2$ crystals as fine grains of average size 3 μm, which interconnect the SiO_2 particles. SEM observation of green moulds make from powder containing 20 wt.% CaO did not reveal any significant difference.

The microstructure of silicate moulds fired at 1200 °C for 1 h are shown in Fig. 3. The bonding particles, containing silicon and calcium as revealed by EDS analysis, are partially welded to SiO_2 particles and both phases have rounded surfaces as a consequence of diffusion during the burnout. The SEM microstructure of traditional moulds after the firing process is shown in Fig. 4. Their morphology substantially alters because of gypsum dehydration.

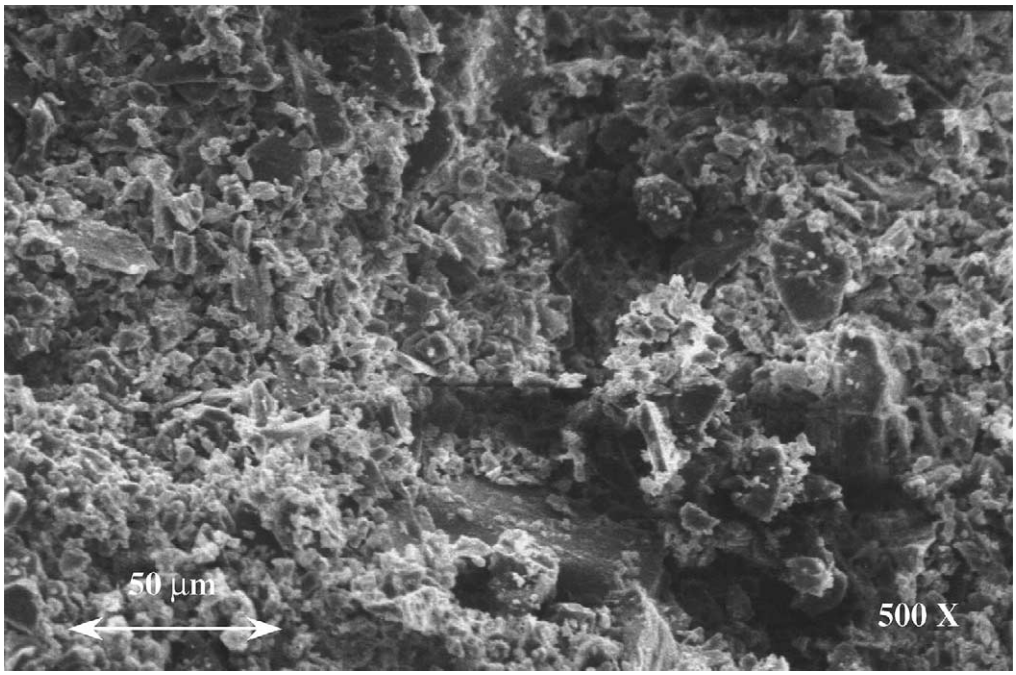

Fig. 3. SEM micrograph of silicate mould (25 wt.% CaO) fired at 1200 °C for 1 h.

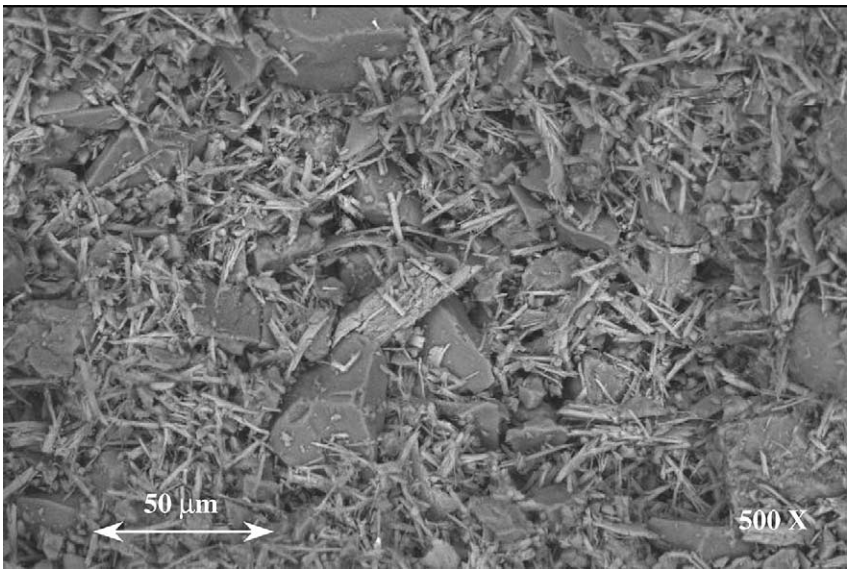

Fig. 4. SEM micrograph of traditional mould (25 wt.% $CaSO_4 \cdot (1/2)H_2O$) fired at 730 °C for 5 h.

Thermal analysis showed striking differences between the traditional and silicate moulds. Fig. 5 shows TG–DTA curves for the traditional green mould. The loss of crystallization water from $CaSO_4 \cdot 2H_2O$ at 140 °C together with two weak endothermic peaks, belonging to α-cristobalite (250 °C) and α-quartz (572 °C) inversions, can be seen. The quartz inversions are of particular interest for the final behaviour of traditional moulds. The two structures of hexagonal SiO_2 differ in symmetry and density [7,8]. At low temperature, α-quartz is stable, but above 572 °C it converts to the more symmetric and less dense β-quartz, with a volume expansion of approximately 1%. The decomposition of anhydrite $CaSO_4$ begins around 900 °C and reaches completion at 1200 °C. However, the temperature of $CaSO_4$ decomposition depends on several factors, such as burnout cycle and carbon impurities from incomplete dewaxing [5].

The TG–DTA analysis of green silicate mould is reported in Fig. 6. The water loss occurs at higher temperature (440 °C). The endothermic process appearing at about 570 °C is the already discussed quartz inversion.

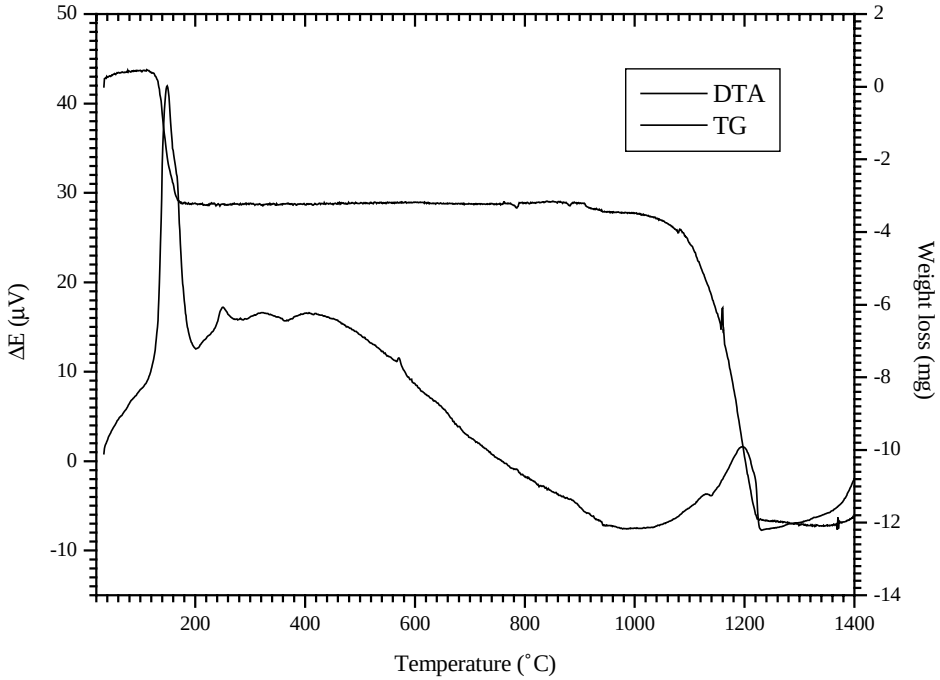

Fig. 5. TG–DTA analysis of traditional mould based on $CaSO_4$ binding phase.

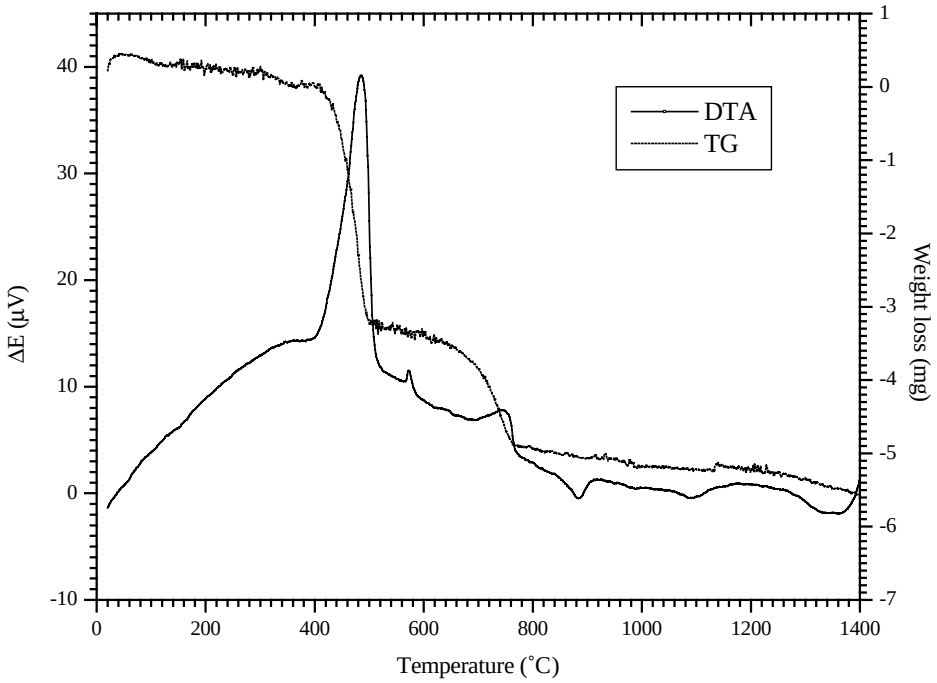

Fig. 6. TG–DTA analysis of new ceramic mould with silicate binding phase.

The weak endothermic peak at about 740 °C is the calcination of $CaCO_3$ traces. These carbonate impurities derive from the CaO reagent. The 10 wt.% loss of H_2O and CO_2 at 1000 °C agrees with the composition specified by the grade certificate. The carbonate decomposition temperature is lower than that for silicate moulds firing, so it cannot cause gas porosity.

The most important feature of the new silicate mould is the thermal stability up to 1400 °C, i.e. over the jewellery casting range. This eliminates the possibility of porosity formation on the surface caused by gas release from component decomposition. The only contribution to inner porosity might reside in alloy shrinkage during solidification.

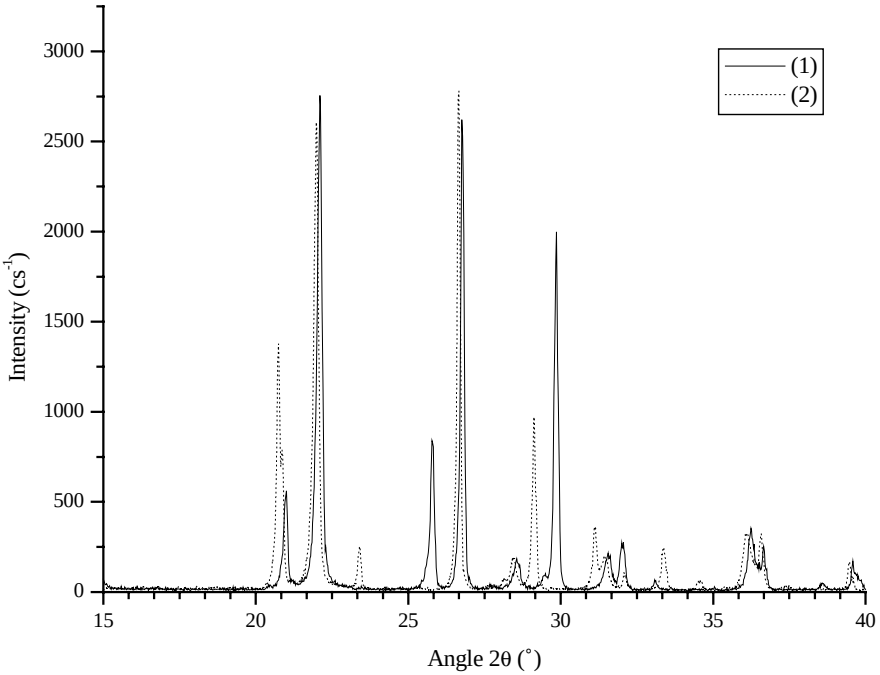

Fig. 7. XRD spectra of traditional powder (1) and its hydration product after setting (2).

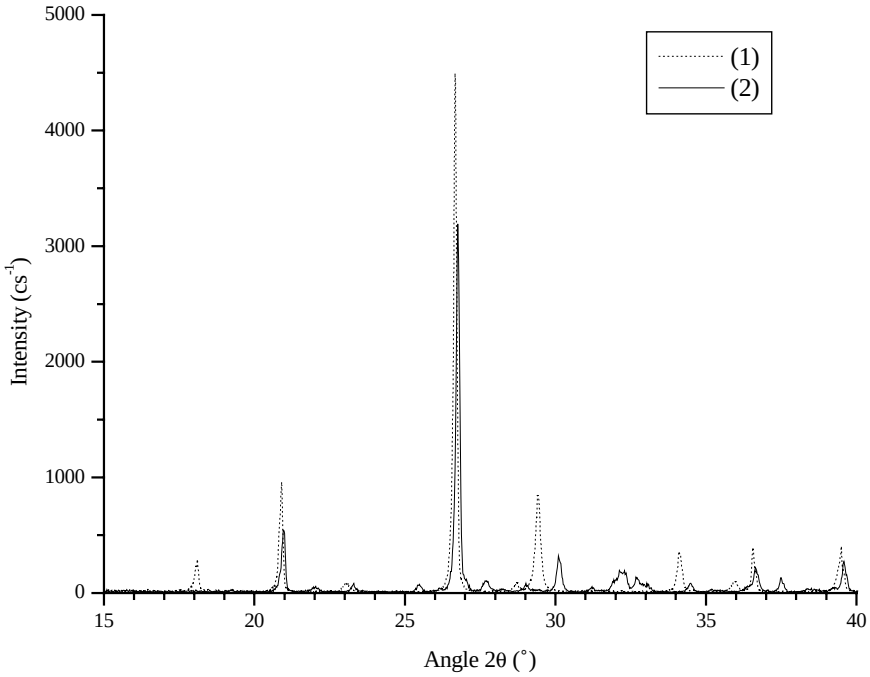

Fig. 8. XRD spectra of new green mould before (1) and after (2) burnout cycle at 1200 °C for 1 h. The peaks of wollastonite and larnite at 30.2° and 32°, respectively are evident.

Thermal analysis, performed on the wax traditionally used for jewellery models, showed a slow decomposition in the range 250–500 °C. At 440 °C, the temperature at which water is released in silicate moulds, the wax has already lost 90% of the original weight by combustion. The new mould is thus able to withstand the mechanical stress induced by thermal expansion of the wax during the dewaxing stage. The traditional mould undergoes water desorption around 140 °C, temporarily losing its mechanical strength just when the wax melts and before its carbonisation.

X-ray spectra for sulphate and silicate moulds (Figs. 7 and 8) show the phase transformations during the burnout. Fig. 7 reports the XRD spectra of starting powder for traditional moulds before and after hydration during

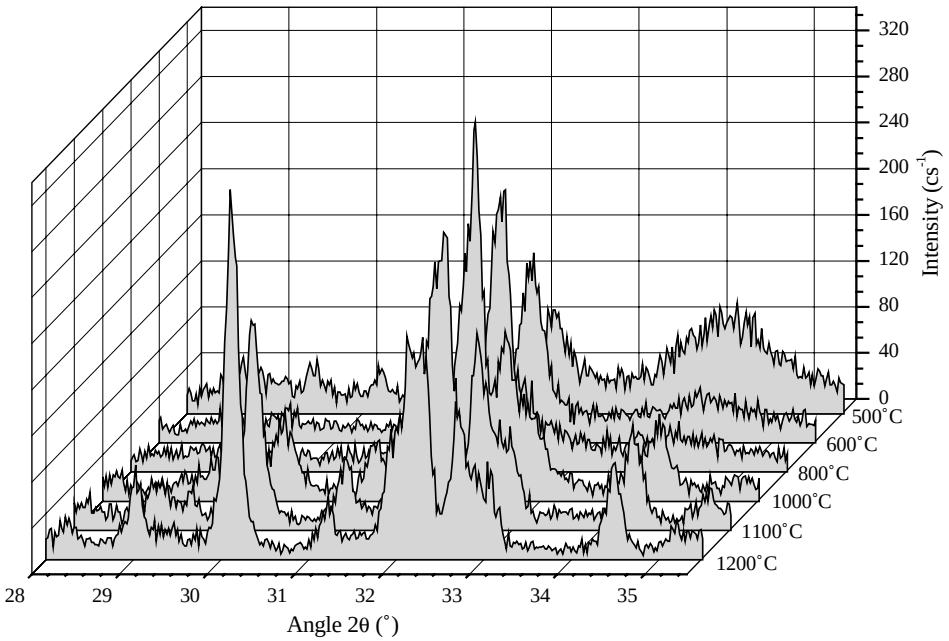

Fig. 9. XRD spectra restricted to silicates angular range as function of temperature. The peaks at 30.2° and 32.2° correspond to $CaSiO_3$ wollastonite and Ca_2SiO_4 larnite.

the investment stage. The quantitative conversion of $CaSO_4{\cdot}(1/2)H_2O$ bassanite [9] into gypsum $CaSO_4{\cdot}2H_2O$ [9] is proved by the disappearance of main bassanite (4 0 0) reflection at around $2\theta = 29.86^\circ$ and the appearance of gypsum (0 2 1 and 0 4 1) peaks at $2\theta = 20.70^\circ$ and $2\theta = 29.13^\circ$, respectively. XRD spectra obtained after the firing stage show the further transformation of gypsum into $CaSO_4$ anhydrite [9].

The hydration and setting of the mixture for silicate moulds leads to the transformation of CaO lime [9] into $Ca(OH)_2$ portlandite [9]. $CaCO_3$ traces from reagent impurity are also detected from (1 0 4) calcite reflection at 29.4°. Fig. 8 reports XRD spectra of silicate moulds before and after burnout. After firing at 1200 °C for 1 h, portlandite is entirely calcined to lime, but the reflections do not appear in the diffraction pattern because of its amorphous state. Indeed, the burnout temperature and duration are too low to enable crystallization of a highly refractory material such as CaO ($T_m = 2614$ °C).

Notwithstanding the breakdown of the $Ca(OH)_2$ scaffold due to its dehydration to CaO, the firing process leads to formation of further bonding phases at the interface amongst SiO_2 particles as evidenced by spectrum 1 in Fig. 8. The diffraction signals at about 30.2° and 32.2° belong to $CaSiO_3$ wollastonite and Ca_2SiO_4 larnite, respectively [9].

The phase transformation in new moulds as a function of firing temperature are summarized in Fig. 9 in which XRD spectra taken on samples fired at six different temperatures ranging from 500 to 1200 °C are reported. The ratio between $CaSiO_3$ and Ca_2SiO_4 changes with the burnout temperature. The peaks of Ca_2SiO_4 were detected above 600 °C while the amount of $CaSiO_3$ sharply increases above 1000 °C. At temperatures higher than 1250 °C, α-cristobalite begins to appear because of α-quartz conversion.

Silicate bonding builds up a thermally resistant network (wollastonite $T_m = 1540$ °C, larnite $T_m = 2130$ °C) that provides a higher mechanical performance compared with the traditional mould. Compression tests were performed on all samples. Results are reported in Table 1. Increased firing temperature produced increased mechanical characteristics because of the higher sintering achieved. The greater CaO content brought a slight decrease of mechanical strength because it leads to larger pores after firing. The wider cavities and porosity derives from the decomposition of the larger amount of $Ca(OH)_2$.

Table 1
Ultimate compression strength, elastic modulus, total porosity and mean pore radius for silicate and traditional moulds

Sample	σ_r (MPa)	E (MPa)	Total porosity (%)	Pore radius (μm)
20% CaO (1000 °C)	0.50 ± 0.06	70.0 ± 8.2	55.7 ± 1.6	1.52 ± 0.17
20% CaO (1200 °C)	1.50 ± 0.12	103.0 ± 10.0	51.4 ± 1.2	1.99 ± 0.11
25% CaO (1000 °C)	0.39 ± 0.07	30.5 ± 5.0	58.1 ± 1.8	1.53 ± 0.19
25% CaO (1200 °C)	1.31 ± 0.14	72.0 ± 9.3	51.9 ± 1.3	2.30 ± 0.15
Traditional	0.11 ± 0.02	29.0 ± 7.5	50.9 ± 1.7	1.30 ± 0.12

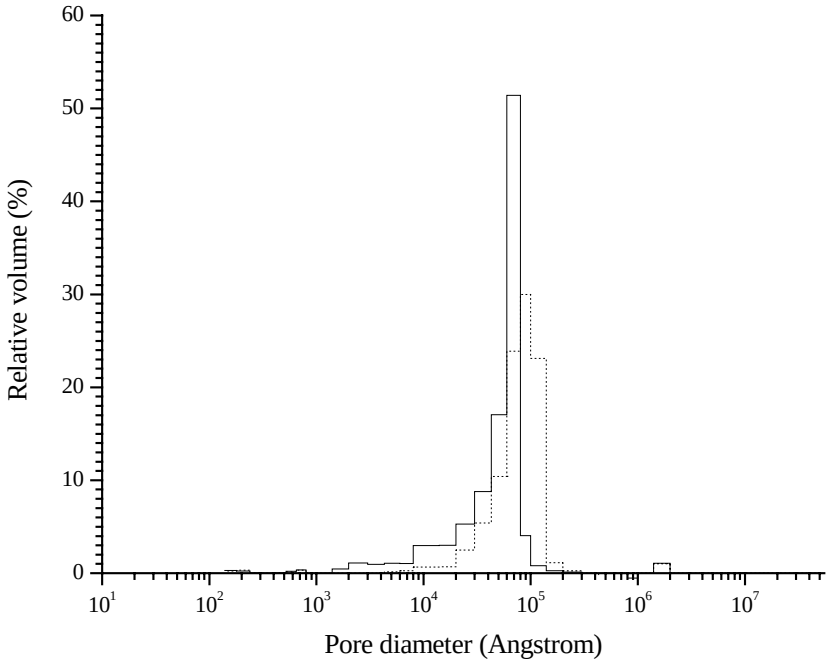

Fig. 10. Pore size distribution of sample with 20 wt.% CaO fired at 1000 °C (solid line) and 1200 °C (dotted line).

The microstructure of ceramic materials depends on the thermal history, so the total porosity of both traditional and silicate casts is related to the firing cycle. Microcasting moulds need a certain degree of porosity to allow degassing during alloy injection, avoiding turbulent filling of the mould. Among the experimental compositions for silicate moulds, those fired at 1200 °C show porosities very similar to that of traditional moulds. In the case of ceramics treated at 1000 °C, the total porosity is higher, but the average pore size is smaller. Fig. 10 reports the pore size distribution of samples containing 20% of CaO sintered at 1000 and 1200 °C.

As expected, firing at higher temperature produced a better sintering, evidenced by the improved mechanical properties and a slight shift of the pore size distribution towards greater values. Results of mercury intrusion analysis are reported in Table 1. In the case of silicate moulds with 25 wt.% CaO fired at 1200 °C for 1 h, a total porosity of 51.9% and a mean pore size of 2.3 μm were measured. From these data a bulk density of 2.47 g cm^{-3} was calculated. The mean values for traditional moulds are very similar: 51.0%, 1.3 μm and 2.53 g cm^{-3}, respectively.

The lower mechanical resistance of 25 wt.% CaO moulds compared with 20 wt.% CaO, at the same temperature, can

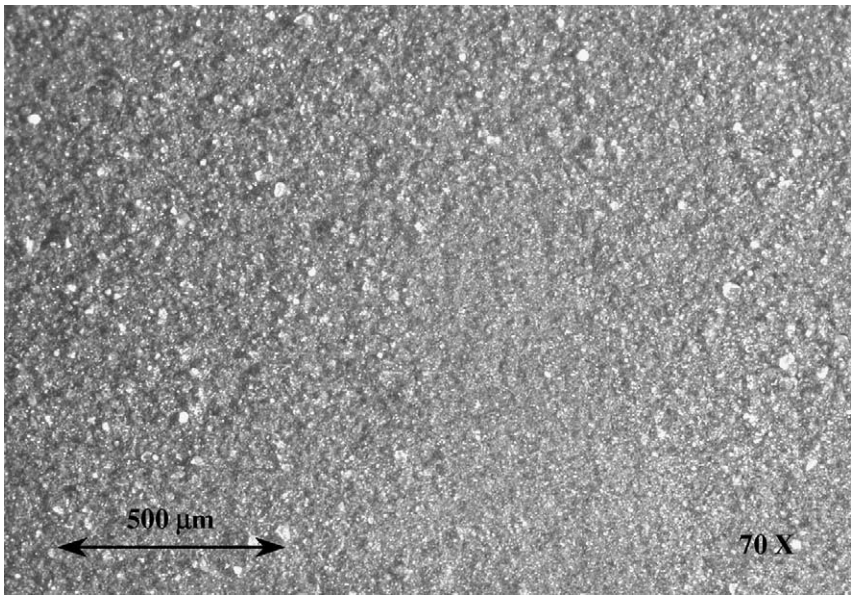

Fig. 11. Surface of silver alloy cast into mould (25 wt.% CaO) fired at 1200 °C (70×).

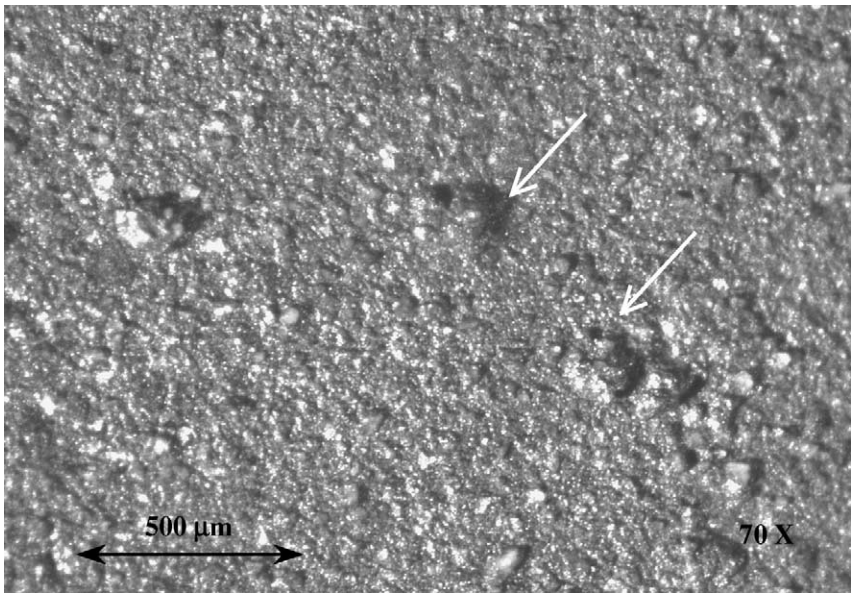

Fig. 12. Surface of silver alloy cast into traditional mould (70×).

be explained on the basis of their higher porosity and larger pores sizes.

To verify the effects of traditional and silicate moulds on the cast alloy, microcasting tests were performed either in traditional or silicate moulds. Stereo optical microscope observation revealed a smooth surface obtained with the silicate moulds (Fig. 11) and the higher roughness and presence of ceramic inclusions in the case of traditional moulds, as evidenced in Fig. 12. Fig. 13 shows an example of Ag 800 microstructure obtained by casting in 20 wt.% CaO mould fired at 1000 °C. Compared with conventional casting (Fig. 14) the grain size of the α phase is just slightly bigger, whereas the eutectic phase (E) is thinner. The amount of ceramic inclusions released by the mould was similar in both cases. The main difference between the two casts is the absence of gas pores in the alloy poured in the new moulds, while a number of such pores were observed in the alloy cast in traditional moulds. As shown in Fig. 15, such pores can be characterized by the presence of a channel connected to the mould, presumably caused by gas release during $CaSO_4$ decomposition.

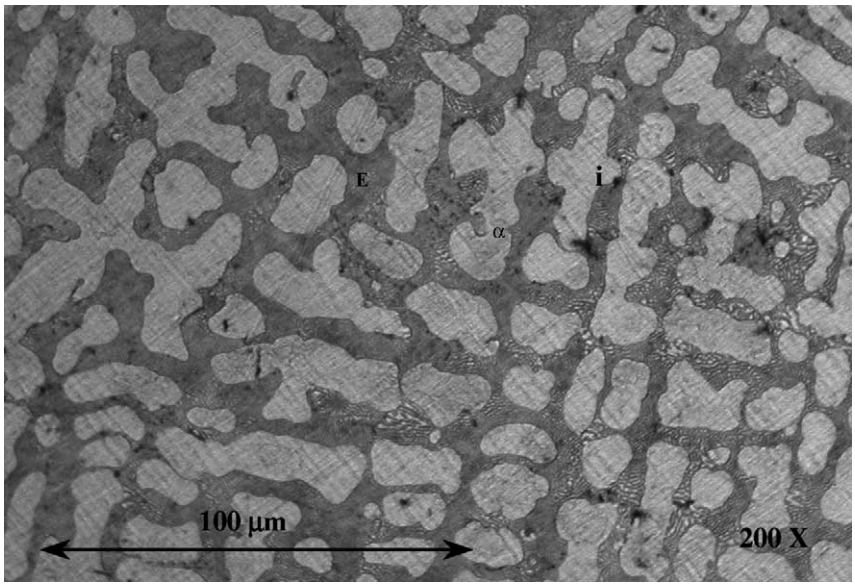

Fig. 13. Example of microstructure of Ag 800 cast into mould (20 wt.% CaO) fired at 1000 °C. The different phases are evidenced by etching the polished surface with chromic acid.

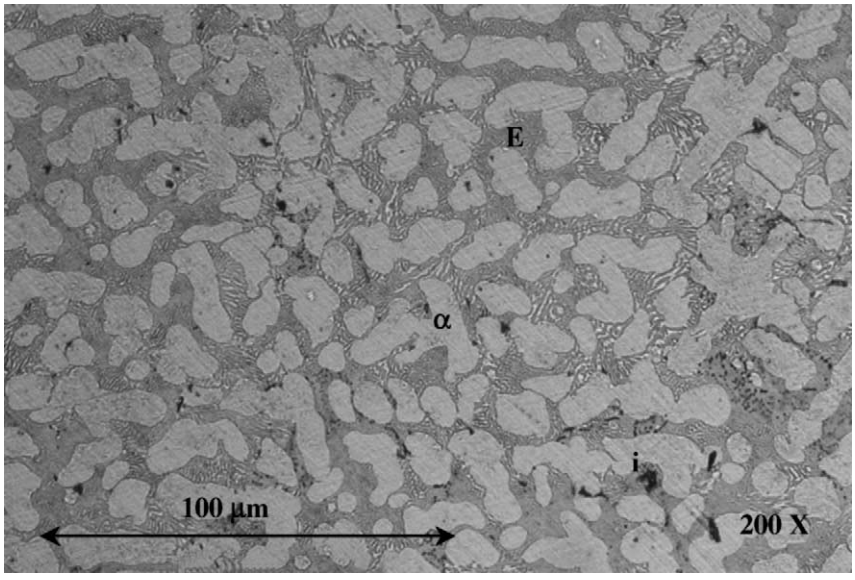

Fig. 14. Microstructure of Ag 800 alloy cast into traditional mould. The different phases are evidenced by etching the polished surface with chromic acid.

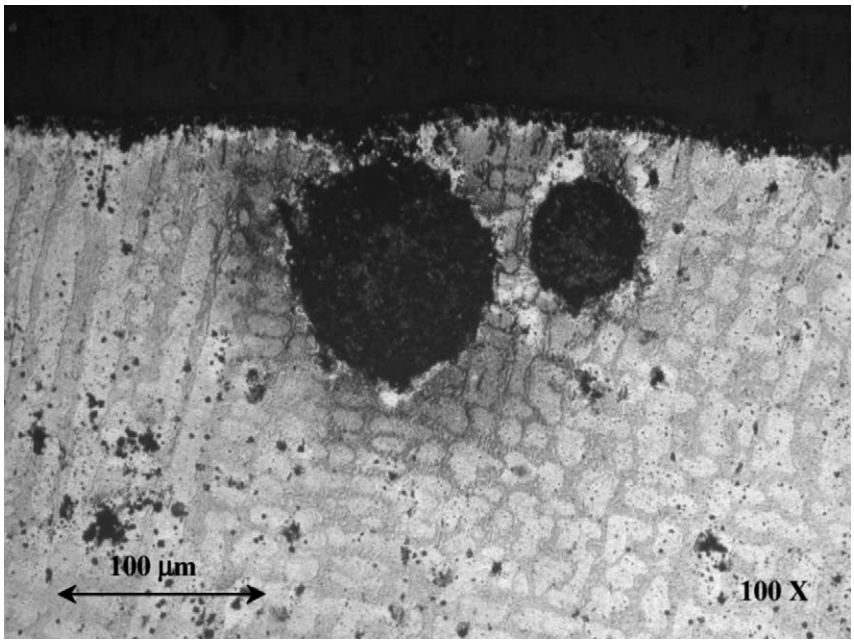

Fig. 15. Typical gas porosity at the alloy edge (Ag 800) caused by $CaSO_4$ decomposition. The different phases are evidenced by etching the polished surface with chromic acid.

4. Conclusions

The novel formulation introduced in the present study shows the possibility of remarkably improving the thermochemical and mechanical performance of traditional moulds for jewellery microcasting. The advance is in the replacement of gypsum phase with a more refractory silicate bonding. The Ca_xSiO_{x+2} species are obtained at temperatures lower than 1000 °C by partial sintering at the interface between SiO_2 quartz and CaO particles. The new moulds showed improved mechanical performance, an increased thermal stability (up to 1400 °C) and a slightly higher porosity with respect to traditional moulds. Increasing CaO content decreases mechanical properties and increases total porosity. On the other hand, increasing firing temperature from 1000 to 1200 °C increases mechanical performance and decreases total porosity. The variation of CaO concentration and of firing temperature permits tailoring mould properties to required performance. Cast tests demonstrated that the use of silicate bonded moulds reduces most of the imperfections derived from the poor thermal stability and low mechanical strength of calcium sulphate bonded moulds and thus decreases production costs.

Acknowledgements

The authors specially wish to thank Prof. Teodoro Valente of the Department of Chemical Engineering at University La Sapienza (Rome), for mechanical tests and master Salvatore Gerardi, director of Goldsmith Arts Academy in Rome, for alloy casting. Particular thanks to masters Augusto Borgna and Antonio Antonelli for priceless assistance. Finally, the authors wish to thank Mr. Michele Zarlenga, mechanic technician at the University of Tor Vergata, for the realization of the several devices used for materials testing.

References

[1] C.W. Corti, in: Proceedings of the XV Santa Fé Symposium on Jewellery Manufacturing Technology, Albuquerque, NM, 2001, pp. 49–70.
[2] D. Pinton, Goldsmith Technology, Gold Editions, Milan, 1999, p. 306.
[3] G.M. Ingo, G. Montesperelli, C. Riccucci, V. Faccenda, A. Bianco, P. Sbornicchia, in: Proceedings of the XV Santa Fé Symposium on Jewellery Manufacturing Technology, Albuquerque, NM, 2001, pp. 241–251.
[4] V. Faccenda, in: Proceedings of the XV Santa Fé Symposium on Jewellery Manufacturing Technology, Albuquerque, NM, 2001, pp. 97–119.
[5] X.J. Zhang, K.K. Tong, R. Chan, M. Tan, J. Mater. Process. Technol. 48 (1995) 603–609.
[6] P. Sbornicchia, G. Montesperelli, G. Gusmano, VI Junior Euromat, New Refractory Ceramic for Jewellery Alloys Casting, F-42, 2002.
[7] H. Yao, I. Hatta, Thermochim. Acta 266 (1995) 301–308.
[8] M.G. Tucker, D.A. Keen, M.T. Dove, Mineralogic. Mag. 65 (4) (2001) 489–507.
[9] JCPDS-ICDD, XRD Spectra Library, 2000.